Quantitative Measurement of Regional Cerebral Blood Flow Using N-Isopropyl-(Iodine-123)p-Iodoamphetamine and Single-Photon Emission Computed Tomography

Gen Takeshita, Hisato Maeda, Kaori Nakane, Hiroshi Toyama, Eiji Sakakibara, Satoshi Komai, Akira Takeuchi, Sukehiko Koga, Mototsugu Ono, and Tsuyoshi Nakagawa

Department of Radiology, Fujita Health University School of Medicine and Mie University School of Medicine, Aichi, Japan

We have developed a quantitative method of measuring regional cerebral blood flow (rCBF) by using N-isopropyl-(iodine-123)p-iodoamphetamine and single-photon emission computed tomography (SPECT). Twenty-five dynamic SPECT images (24 sec/scan) were collected immediately after tracer injection using a ring-type SPECT system and the accumulation curve (C(t)) was obtained. The time-activity curve corresponding to the arterial blood activity curve was used as B(t). The latter curve was calculated from the lung time-activity curve monitored during scanning and corrected by the actual activity obtained by one-point blood sampling 5 min after tracer injection. The octanol extraction ratio during scanning was considered to be constant and taken as the value measured 5 min after tracer injection (E). The uptake constant (K) per pixel was calculated by the least squares fitting method as the slope of the linear relationship in which $C(t)/E \times B(t)$ was plotted against $E \times \int_0^t B(\tau)d\tau/E \times B(t)$. Functional maps of rCBF values were obtained on a 64 × 64 matrix by calculating the uptake constant per pixel and the cross calibration factor (CF) between the SPECT system and a well counter ($rCBF = K \cdot CF \times 100$).

J Nucl Med 1992; 33:1741–1749

The distribution of N-isopropyl-(iodine-123)p-iodoamphetamine [^{123}I]IMP (*1,2*) is considered to represent the regional cerebral blood flow (rCBF) and to resemble a microsphere model in the early period after injection. We have developed a new technique for the quantitative measurement of rCBF by using [^{123}I]IMP SPECT and have used it to obtain functional maps of rCBF values. This method involves determining the uptake constant (*3,4*) in the period where the microsphere model can be applied. To determine the uptake constant for the brain, accurate input and output values are necessary. For this purpose, we propose a simplified method that simulates the arterial blood activity curve by using a lung time-activity curve and one-point sampling of arterial blood.

Received Nov. 19, 1991; revision accepted Dec. 5, 1992.

For reprints contact: Gen Takeshita, MD, Dept. of Radiology, Fujita Health University School of Medicine, 1-98, Dengakugakubo, Kutsukake, Toyoake, Aichi, Japan.

Theory

If the washout of [^{123}I]IMP from the brain can be considered negligible in the period immediately after intravenous injection, the amount of tracer scanned in the brain can be determined as follows

$$C(t) = F \cdot B(t)\{1 - E(t)\} + K \cdot \int_0^t B(\tau) \cdot E(\tau)d\tau, \quad \text{Eq. 1}$$

where B(t) is the change in arterial blood activity as an input function, E(t) is the change of the ratio of the lipophilic component of B(t), the so-called octanol extraction ratio ($0 < E(t) < 1$), F is the background activity (mainly in the blood pool in the brain due to the hydrophilic component of B(t)), C(t) is the sum of the brain activity as an output function, and K is the uptake constant which represents the fraction of the activity in the lipophilic component of B(t) that is taken up by the brain per unit time. Equation 1 is converted to:

$$\frac{C(t)}{B(t)E(t)} = F\frac{1 - E(t)}{E(t)} + K \cdot \frac{\int_0^t B(\tau)E(\tau)d(\tau)}{B(t)E(t)}. \quad \text{Eq. 2}$$

If E(t) is constant (E), Equation 3 is as follows:

$$\frac{C(t)}{E \times B(t)} = F\frac{(1 - E)}{E} + K \cdot \frac{E \times \int_0^t B(\tau)d\tau}{E \times B(t)}. \quad \text{Eq. 3}$$

If $C(t)/E \times B(t)$ is plotted against $E \times \int_0^t B(\tau)d\tau/E \times B(t)$, the relationship between $C(t)/E \times B(t)$ and $E \times \int_0^t B(\tau)d\tau/E \times B(t)$ should be linear with a slope of K and an intercept on the Y axis at $F(1 - E)/E$ at a time before washout of [^{123}I]IMP from the brain occurs. K thus represents a relative index of the cerebral blood flow.

In clinical studies using dynamic SPECT, the value of C(t) can be determined as the change in the reconstructed counts per unit time (reconstructed counts/pixel/unit time) and B(t) can be measured as the activity of the arterial blood per unit volume by a well counter (well cpm/unit volume). K is thus represented as:

$$\frac{\text{reconstructed counts/pixel/unit time}}{\text{well cpm/unit volume}}.$$

A cross calibration factor (CF) is necessary to adjust the units in the two different measurements, and this is defined as the reconstructed counts per pixel in SPECT images against the values determined by a well counter per unit gram, which is measured using an aqueous solution with ^{123}I solution. Thus, CF is expressed as:

$$\frac{\text{well counts per minute/unit gram}}{\text{reconstructed counts/pixel}}$$

If the density of brain tissue is taken as equal to that of water, rCBF values can be calculated as follows:

$$\text{rCBF} = \text{K} \times \text{CF(unit volume/unit gram/unit time).} \quad \text{Eq. 4}$$

We have proposed a simplified method for determining the arterial blood activity curve by calculating B(t) values using the lung time-activity curve (lung TAC), thus avoiding the need for frequent sampling of arterial blood. The principle of this calculation is as follows: when [^{123}I]IMP is injected intraveneously, first-pass extraction in the lungs is very high and subsequently the tracer is released to the brain through the left heart (*5*). The curve which is obtained by the subtraction of ongoing lung TAC values from the peak lung TAC value shows the sum of the activity of [^{123}I]IMP which is released from the lungs into arterial blood. A differentiated curve derived from this subtraction curve thus simulates the changes of [^{123}I]IMP in arterial blood. The differentiated curve is corrected by the actual activity obtained from a single sample of arterial blood (one-point sampling).

MATERIALS AND METHODS

A new method for quantifying rCBF using [^{123}I]IMP SPECT was evaluated in healthy volunteers and patients, using ^{133}Xe inhalation SPECT studies as the reference standard. Informed consent was obtained before examination in all cases.

A ring-type SPECT system (Headtome SET-031, Shimadzu Corp., Japan) was used (*6*). It consists of three detector rings: three SPECT images with a 35 mm gap can be obtained. Data acquisition was performed every 12 sec with a 64 × 64 matrix and tomographic images were reconstructed using the filtered backprojection method. The energy window level was adjusted to 135–183 keV (±15%) for the photopeak of ^{123}I (159 keV) and to 74–100 keV (−8 ~ 23%) for the photopeak of ^{133}Xe (81 keV). FWHM of the spatial resolution for a high-sensitivity collimator was 19.2–20.4 mm, and 12.0–12.4 mm for a high resolution collimator for the line source of ^{123}I in air. The slice thickness at FWHM was 26.0–29.0 mm for the high-sensitivity and 17.5–19.0 mm for the high-resolution collimator in the case of ^{123}I. FWHM for the ^{133}Xe line source in air using an HS collimator was a spatial resolution of 19.2–20.6 mm. Attenuation correction was automatically performed by calibration of the counts in each detector with those calculated from the geometrical distribution of activity using a 20 cm diameter cylindrical phantom, as reported by Kanno et al. (*6*).

The term "frame" means a single 24-sec interval described as follows. Twenty-five dynamic SPECT images with a frame time of 24 sec as C(t) were obtained with a HS collimator in a 10-min period after the intravenous injection of 222 MBq (6 mCi) of [^{123}I]IMP (111 MBq in healthy volunteers). Three SPECT images were obtained on the slices 20, 55 and 90 mm above the orbitomeatal (OM) line. The OM line was determined in each case by using a slit light beam incorporated into the SPECT system.

The lung TAC was also monitored on the right anterior chest wall at 3-sec intervals, using a scintillation probe incorporated into the SPECT system. The probe was collimated in the right upper lung field using a 1-mm thick Pb shield with a 6 mm diameter hole. The energy window level of the probe was also adjusted to 135–183 keV for the ^{123}I photopeak.

The following analysis was performed using a personal computer (NEC 9801-RA) after the data from dynamic SPECT images and lung TAC were entered onto a floppy disk. Figure 1 shows the procedures used to produce the arterial blood activity curve at 24-sec intervals in a healthy volunteer. The original lung TAC determined at 3-sec intervals (Fig. 1A) had a sharp peak. After the peak, the curve decreased rapidly in the early period and gradually in the late period. The falling limb of the lung TAC showed fine wavering caused by the rebreathing. The lung TAC was fitted by bi-exponential curves for the part which showed

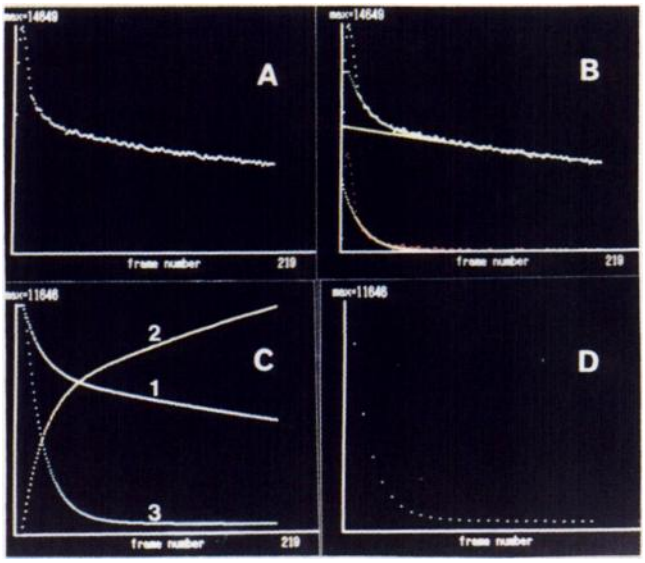

FIGURE 1. (A) The original lung time-activity curve obtained at 3-sec intervals in a healthy volunteer. (B) Two-compartment fitting of exponential curves to the original curve. (C) The arterial blood-activity curve (3) calculated by differentiation of curve (2), which was obtained by subtraction of the fitted lung time-activity curve (1) from its peak value. (D) The calculated arterial blood activity curve obtained at 24-sec intervals. All images are from the monitor and show relative counts on the y-axis and a series of frames on the x-axis.

these fluctuations, excluding the peak which was considered to reflect the tracer moving through the pulmonary vasculature (fitted Lung TAC, Fig. 1B). The peak of the fitted lung TAC was set at the fifth point (15 sec after tracer injection). A subtraction curve after the peak was then obtained by subtracting the fitted lung TAC from the peak of the fitted lung TAC; and the calculated arterial blood activity curve was obtained by differentiation of the subtraction curve (Fig. 1C). The peak of the calculated arterial curve was set at the fifth point identically with the fitted lung TAC and the value before the peak was considered as zero value. The calculated arterial blood activity curve was then converted to the curve with a time interval of 24 sec (Fig. 1D) as B(t). One-point sampling of arterial blood was performed at 5 min after tracer injection and the calculated curve was corrected by actual arterial blood activity. Octanol extraction of the arterial blood sample was done as soon as possible after its collection and the value of E in Equation 3 was decided as the ration at 5 min after tracer injection.

TABLE 1
List of Patients

Patient no.	Sex	Age	Diagnosis	CT Findings	Comment
1	M	54	infarct	rt lacune	rt ICO
2	M	54	vertigo	normal	
3	M	34	SCD	atrophy	
4	M	59	vertigo	atrophy	
5	F	68	ICH	scar after ICH	2 yr after onset
6	F	42	Moyamoya	watershed infarct	
7	M	61	infarct	rt lacune	
8	M	63	infarct	LD positive	rt ICO
9	M	46	vertigo	rt lacune	
10	M	63	cardiopathy	normal	
11	M	28	myopathy	normal	
12	M	75	infarct	rt lacune	rt ICO
13	F	75	Parkin-sonism	atrophy	
14	M	75	infarct	rt lacune	rt ICO

ICO = internal carotid artery occlusion; SCD = spinocerebellar degeneration; ICH = intracerebral hemorrhage; LD = low density area; and lacune = small infarcts in the basal ganglia, thalamus and deep while matter.

In two subjects, the arterial blood samples were withdrawn every minute and the calculated arterial blood activity curve was compared with the actual changes of blood tracer activity. The changes of the octanol extraction ratio during scanning were also obtained. The CF for calibration between mean reconstructed counts in SPECT images and the value for 1 g water obtained with a well counter was measured using a 20 cm diameter cylindrical phantom filled with an aqueous ^{123}I solution. The density of the brain was defined as equal to that of water (1.0 g/ml).

C(t) was defined as the change of reconstructed counts per pixel every 24 seconds in a ROI of the serial dynamic SPECT images. When $C(t)/E \times B(t)$ was plotted against $E \times \int_0^t B(\tau)d\tau/E \times B(t)$, the B(t) values after the second frame and C(t) values subtracted from that of the first frame were used, because the B(t) value obtained in the first frame by our fitting method was believed to be unreliable. The slope of the straight line (K) which reflected the linear relationship between $C(t)/E \times B(t)$ and $E \times \int_0^t B(\tau)d\tau/E \times B(t)$ was determined by the least squares fitting method. The range of fitting was decided as the period in which the least square deviated values were significantly low in the healthy volunteers and was applied to determining K values in

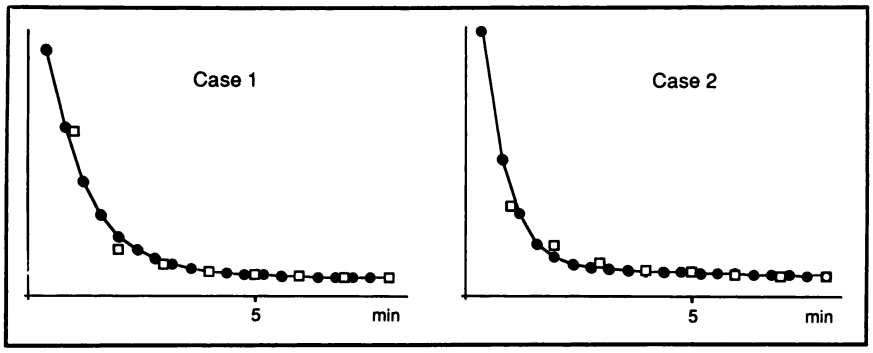

FIGURE 2. The arterial blood-activity curves calculated in two subjects and compared to the actual blood activity in samples withdrawn every minute in the first 8-min period (closed circles = calculated values and open squares = actual values).

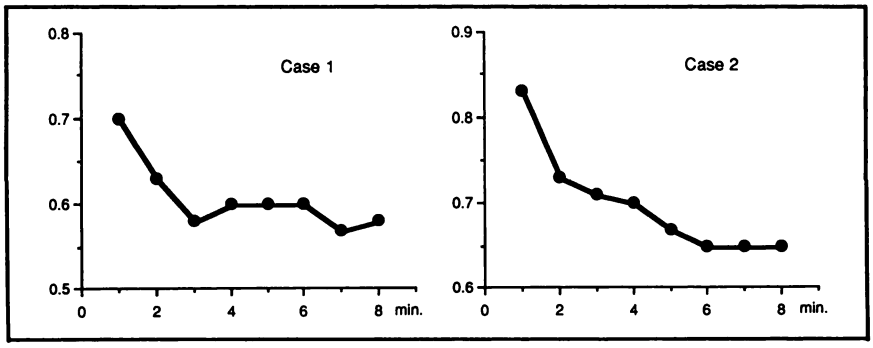

FIGURE 3. Changes of the octanol extraction ratio during the first 8 min in two subjects.

the patients. Then rCBF values ($rCBF_K$) were calculated as follows:

$$rCBF_K = K \times CF \times C \times 100 \text{ (ml/100 g/minute)} \quad \text{Eq. 5}$$

where C is the constant by which the unit of time was converted to 60 sec from 24 sec. The K values for each pixel were determined and functional maps which showed the $rCBF_K$ values were displayed on the color monitor with a 64 × 64 matrix.

Xenon-133 inhalation SPECT studies were performed as the reference standard. Approximately 1.85 GBq(50 mCi) of ^{133}Xe gas was administered by rebreathing through a mouth piece for one min. During this period and the subsequent 7 min of ^{133}Xe washout, a series of eight consecutive ^{133}Xe distribution maps of the brain was taken each of 1 min duration using an HS collimator. The rCBF values were then calculated by the sequential picture method of Kanno and Lassen (*7,8*).

Four healthy volunteers and the 14 patients summarized in Table 1 were studied. There were one female and three male volunteers aged 25–37 yr. $rCBF_K$ values for the cortex and the mean $rCBF_K$ values for the cerebral hemispheres were evaluated on functional maps drawn at 55 and 90 mm above the OM line. The rCBF values of all patients were also measured by ^{133}Xe inhalation SPECT studies as the reference standard. The correlation between $rCBF_K$ values and the rCBF values determined by ^{133}Xe inhalation SPECT was evaluated in the 14 patients for the ROIs placed over both cerebral hemispheres on slices at 55 and 90 mm above the OM line. The $rCBF_K$ and rCBF data by ^{133}Xe were not corrected for the arterial blood CO_2 concentration.

In a patient with infarcts, the $rCBF_K$ and rCBF values were compared with the low density areas shown on CT. Lesions for which ^{133}Xe rCBF maps showed low-perfusion areas without massive low density areas on CT, as in three cases where there was internal carotid artery occlusion (ICO), were compared with the conventional SPECT images obtained from 20 min after the injection ^{123}I over a 15 min period using an HR collimator.

RESULTS

The curve calculated as B(t) well simulated the actual changes of arterial blood tracer activity in the period from 1–8 min after injection in the two subjects as shown in Figure 2. The changes of octanol extraction ratios in these two subjects are shown in Figure 3. The differences of the ratios in the first 5 min period ranged from 0.10–0.13.

Figure 4 shows dynamic SPECT images obtained with a frame of 24 sec and the change of reconstructed counts obtained as C(t) for the ROI over the cerebral hemisphere in a volunteer. In the first frame the value of the reconstructed counts in the brain was too small to determine, but after the second frame the SPECT images had an adequate counts value.

The uptake constant for the ROI of the volunteer was calculated from the slope of the straight line obtained when $C(t)/E \times B(t)$ was plotted against $E \times \int_0^t B(\tau)d\tau/E \times B(t)$ after the second frame, as shown in Figure 5. Table 2 shows the changes of the least square deviated values and the $rCBF_K$ values fitted in the time interval from the second frame (the first plot) to fifteenth frame (the fourteenth plot) for the ROI placed over the cerebral hemispheres 90 mm above the OM line in two healthy volunteers. As shown in Figure 6, the least square deviated values fitted from the second frame were significantly larger in the two volunteers than those fitted from the third, fourth and fifth frames, which showed almost constant and low values in all the volunteers. The least square deviated values showed a marked increase for the fits ending after the eleventh or twelfth frames. Therefore, the start of linear fitting was set as the third frame (the second plot) and the end of linear fitting as the ninth frame (the eighth plot). The $rCBF_K$ values showed little difference for the fits starting from the third frame and ending before the ninth frame, as shown in Table 2. Functional maps of $rCBF_K$ values per pixel were obtained with linear fitting from the third to the ninth frame in the healthy volunteers and patients.

In the functional maps of the volunteers, the alignment of the cortex was clearly visualized on the slices obtained 55 and 90 mm above the OM line, although the basal ganglia, thalamus, and centrum semiovale were not sharply demonstrated. Functional maps for a healthy volunteer are shown in Figure 7. In the four normal volunteers, $rCBF_K$ values (ml/100 g/min) for the 3 × 3 pixel ROIs in the cortex ranged from 61 to 86 with a mean value of 70.1 ± 7.1. The mean $rCBF_K$ values for the cerebral hemispheres ranged from 47–65 with a mean value being 54.8 ± 5.8 (Table 3).

In the 14 patients, the mean $rCBF_K$ values for the cerebral hemispheres correlated well with the rCBF values obtained by ^{133}Xe inhalation SPECT, as shown in Figure 8 ($y = 1.03x - 1.85$, $r = 0.89$, $p < 0.01$).

In a patient with low-density areas in the territory of the anterior and middle cerebral arteries on brain CT (Patient 8), $rCBF_K$ was 13 ml/100 g/min and rCBF was 15 by ^{133}Xe studies in the ischemic region, as compared to 37 ($rCBF_K$) and 44 (rCBF by ^{133}Xe) in the contralateral region (Fig. 9). In three patients who had ICO with small low-density areas in the basal ganglia and/or deep white matter but without massive low-density areas in the cortex, the hypoperfused areas revealed by ^{133}Xe inhalation SPECT studies were visualized more clearly using the functional maps than with the conventional [^{123}I]IMP images (Patients 1, 12, 14). Patient 12 had right-sided ICO and brain CT showed only small low-density lesions in the right basal ganglia, but hypoperfused areas in the right frontal lobe were clearly shown on the functional maps and ^{133}Xe rCBF images, while these areas were less distinct in the conventional [^{123}I]IMP images (Fig. 10). In this case the hypoperfused areas in the territory of the middle cerebral artery had a mean $rCBF_K$ value of 33 ml/100 g/min, while it was 39 in the contralateral cortex.

DISCUSSION

The early distribution of [^{123}I]IMP resembles a microsphere model and washout from the brain is reported to be very small in the first ten minutes after injection (*9, 10*). It is thus possible that Equation 1 can be applied to

[^{123}I]IMP SPECT in the period immediately after injection and that the uptake constant (K) represents rCBF.

The reconstructed images obtained at 24-sec intervals by dynamic SPECT using a ring-type system provided sufficient counts even in the period immediately after tracer injection. We shall now discuss how accurately the SPECT images represented the actual distribution of [^{123}I] IMP. One of the most difficult problems in performing quantitative measurement by SPECT is the accuracy of attenuation correction. In our SPECT system the attenuation correction was performed using a 20-cm diameter cylindrical phantom and the reconstructed counts in the human brain were not always actually corrected. However, in our experimental study using a brain phantom and an HS collimator, the reconstructed counts in the peripheral region on the short axis were overestimated by only 2%–3% in relation to those for the long axis. We considered that the attenuation correction in the cortex was satisfactory, although the accuracy of the correction could not be established for the deep-seated structures because of low spatial resolution. It is also difficult to overcome the influence of scatter (*6*), which reduces the accuracy of quantitative values. To decrease the effect of scatter in ^{133}Xe studies, the lower energy window level was adjusted to 75 keV (−8%) for the ^{133}Xe photopeak. Scatter is a common problem in ^{123}I quantitative studies but its effect is considered to be less in [^{123}I]IMP images than in ^{133}Xe images. The factor which has a great influence on the measurement of regional tracer concentrations in tomographic images is the relationship between the size of an object and the spatial resolution of the system, as mentioned by Hoffman et al. (*11*). In the current study, ROIs were made large enough for FWHM in the cerebral hemispheres to minimize the effects of low spatial resolution when the mean $rCBF_K$ and mean rCBF values were evaluated by ^{133}Xe. The quantitative values for the cortex were evaluated in the young healthy volunteers without any loss of brain volume by using relatively small ROIs which were limited to the cortex.

To obtain B(t) values, frequent arterial blood collection at 24-sec intervals is not acceptable in clinical studies, so a simplified method which required only one-point sampling of arterial blood was tested. In the two subjects tested, the actual arterial blood activity changes every minute were well simulated by the curves calculated from their lung TAC data. B(t) values immediately after injection were not identified with the actual activity and the B(t) values in the first frame were considered as unreliable. However, after the second frame, the calculated B(t) values were considered to represent the actual changes, because the fitted line intercepted the y-axis at nearly zero in most cases when the ROI was placed over the brain, and the high blood:brain partition coefficient of [^{123}I]IMP made the background activity negligible ($F \fallingdotseq 0$ in Equation 3).

Changes of the octanol extraction ratio indicated the in vivo changes of [^{123}I]IMP with time from a lipophilic tracer which could bind to the brain to a hydrophilic metabolite. We considered the ratio constant at the 5 min value because the ratios showed a little change in the period from 1 to 5 min, in which linear fitting to determine the K value was done. In addition, the blood tracer concentration was relatively stable at 5 min and changes of the arterial blood activity were thought to be slight during blood collection, even if this was not done smoothly.

When $C(t)/E \times B(t)$ was plotted against $E \times \int_0^t B(\tau)d\tau / E \times B(t)$ after the second frame (Fig. 5), both parameters had an almost linear relationship in the early period after tracer injection. A linear fit by the least squares fitting method was obtained from the third to the ninth frame, a time interval of approximately 1–4 min after tracer injection. In the later period (up to 10 min), the least square deviated values showed a marked increase and the plots gradually deviated from the straight line. This suggests that washout of [^{123}I]IMP from the brain had begun even in the first ten min after its injection. The period for which the straight line can be correctly fitted may vary with the type of brain lesion present, because washout of [^{123}I]IMP occurs more rapidly as brain perfusion increases and more slowly as perfusion decreases. In this study, the period of correct fit was obtained from an analysis of healthy volunteers and was considered to be applicable to hypoperfused lesions, which are most important for clinical diagnosis because hypoperfusion delays tracer washout. However, with hyperperfused lesions the washout cannot be negligible in the period immediately after injection, so the possibility that $rCBF_K$ values may underestimate the actual rCBF must be noted.

Positron emission tomography (PET) has revealed that the normal rCBF is approximately 60–80 ml/100 g/min in the gray matter and that 40–50 ml/100 g/min is the mean hemispheric blood flow (*12–16*). In our young healthy volunteers, the mean $rCBF_K$ was 71.7 in the cortex and 54.8 for the cerebral hemispheres (ml/100 g/min). These values were in agreement with the rCBF data obtained by PET and also in agreement with the results of multi-probe ^{133}Xe studies and ^{133}Xe inhalation SPECT studies. A cortical flow of 64 ± 9 ml/100 g/min was obtained by Olesen et al. (*17*) using the initial slope of the clearance of an intra-arterial injection of tracer: 74.5 and 54.7 ml/100 g/min were respectively obtained for the cortex and the averaged hemisphere by Orbist et al. (*18*) using the three-compartment analysis of inhaled ^{133}Xe: 72 ± 12 ml/100 g/min was obtained as the mean gray matter flow by Devous et al. (*19*): and 49–61 ml/100 g/min was the hemispheric flow determined by Lauritzen et al. (*20*).

Celecia et al. (*16*) reported that the mean rCBF of infarcted areas with a decreased density was seen at 14 ml/100 g/min, and Lenzi et al. (*21*) reported that a decrease of rCBF below 20 ml/100 g/min correlated with a poor clinical outcome in PET studies. In a SPECT study using ^{133}Xe inhalation, Lassen et al. (*22*) showed that ischemic regions had a flow rate of approximately 20 ml/100 g/

TABLE 2

The Least Squares Deviated Values and the $rCBF_K$ Values Obtained in Two Healthy Volunteers in the Fits Starting from the Second to Fifth Frame and Ending Before the Fifteenth Frame

Subject 1													
End	3	4	5	6	7	8	9	10	11	12	13	14	15
Start 2	0	0	0	3	12	21	23	25	48	87	127	195	268
	59	58	57	56	55	54	54	54	53	52	51	50	49
3		0	0	2	10	18	19	20	41	77	112	174	238
		59	58	57	55	54	54	53	52	51	50	49	47
4			0	1	7	12	11	11	28	59	86	136	186
			57	56	54	53	52	52	51	50	49	47	46
5				0	2	3	3	2	15	37	56	90	123
				54	52	51	51	51	49	47	46	44	43
Subject 2													
End	3	4	5	6	7	8	9	10	11	12	13	14	15
Start 2	0	26	68	92	109	126	127	124	126	133	146	166	212
	82	68	59	55	52	50	49	48	48	47	46	46	45
3		0	7	10	13	19	19	18	19	25	342	50	89
		57	52	50	48	47	47	47	46	46	45	45	44
4			0	0	0	3	2	2	3	7	14	27	61
			48	47	47	46	46	46	46	45	45	44	44
5				0	0	2	1	1	2	5	11	23	54
				47	46	45	46	46	45	45	45	44	44

Upper numbers are least square deviated values (relative values) and bottom numbers are $rCBF_K$ values (ml/100 g/min).

min. In our patient with a massive cerebral infarction, the low perfusion areas where CT showed a low density had an $rCBF_K$ of 13 ml/100 g/min, as compared to 37 in the contralateral area. Thus, the $rCBF_K$ value in the ischemic region was in agreement with the data mentioned above.

Areas of low perfusion without any evidence of low density on CT were less distinct on conventional [^{123}I]IMP images than on functional maps in three cases of ICO. It is possible that the washout of [^{123}I]IMP from the brain had already occurred in the period when conventional images were obtained and that washout from healthy tissue may be relatively larger than that from low perfusion areas, because washout is considered to increase along with rCBF. The functional maps used in this study were based on early dynamic images and sensitively allowed the detection of areas with a mild reduction of perfusion despite the lower spatial resolution of an HS collimator (*23*).

There are several advantages of our quantitative method as compared to ^{133}Xe inhalation SPECT. First, ^{133}Xe gas can be used only once a week, while [^{123}I]IMP can be delivered 5 days a week. Although the FWHM values of the spatial resolution for the line source in air were almost equal for both ^{123}I and ^{133}Xe, ^{123}I was considered to be superior to ^{133}Xe because of its lesser effect on scatter during in vivo quantitative SPECT measurements. ^{133}Xe inhalation studies cannot be performed on unconscious patients following neurosurgery, or when anesthetic agents are required during the examination. After the quantitative study was performed, conventional SPECT in [^{123}I]IMP images were obtained with the HR collimator. In addition,

TABLE 3

$rCBF_K$ Values Obtained in Four Healthy Volunteers (ml/100 g/min)

Subject no.	Sex	Age	Slice	Hemisphere		Frontal		Temporal		Occipital		Parietal	
				Right	Left	Right	Left	Right	Left	Right	Left	Right	Left
1	M	31	55 mm	59	54	69	61	68	60	73	66		
			90 mm	57	56	70	72					73	77
2	M	37	55 mm	53	47	74	63	73	68	68	62		
			90 mm	52	47	65	60					65	65
3	M	30	55 mm	51	46	76	72	75	68	77	59		
			90 mm	53	53	68	65					65	68
4	F	25	55 mm	62	59	77	69	83	65	71	73		
			90 mm	63	65	84	86					83	78
Mean		30.8		54.8 ± 5.8		70.7		70.0		68.6		70.5	

55 and 90 mm = the slice above the OM line.

The mean $rCBF_K$ value in the cortex was 70.1 ± 7.1 ml/100 g/min.

our method may possibly be used with a gamma camera rotating type SPECT system, if SPECT images can be obtained at least every minute with a dual- or triple-headed camera.

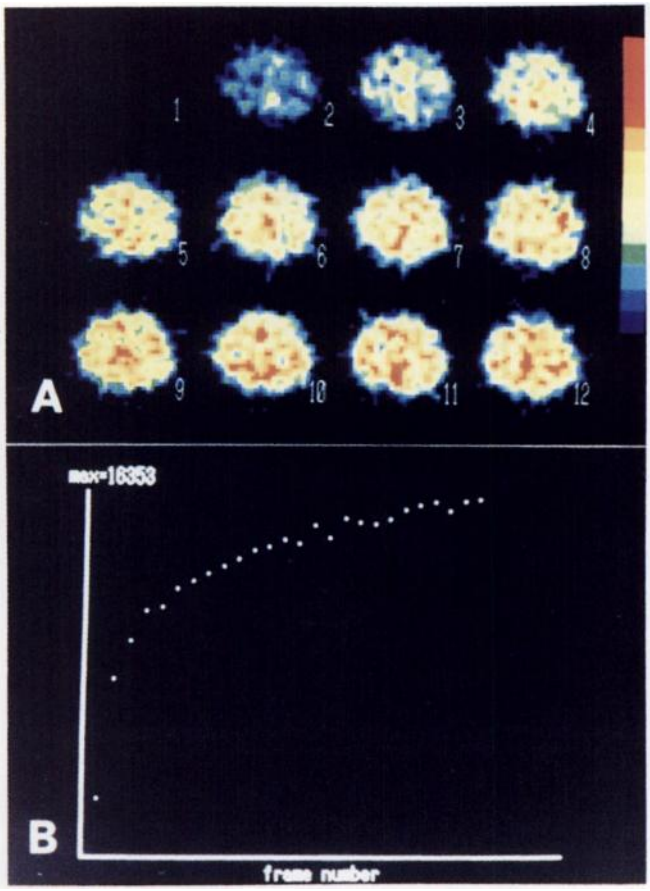

FIGURE 4. Twelve serial dynamic SPECT images (A) and the changes of the reconstructed counts on the ROI placed over a cerebral hemisphere (B) in the same subject as shown in Figure 1.

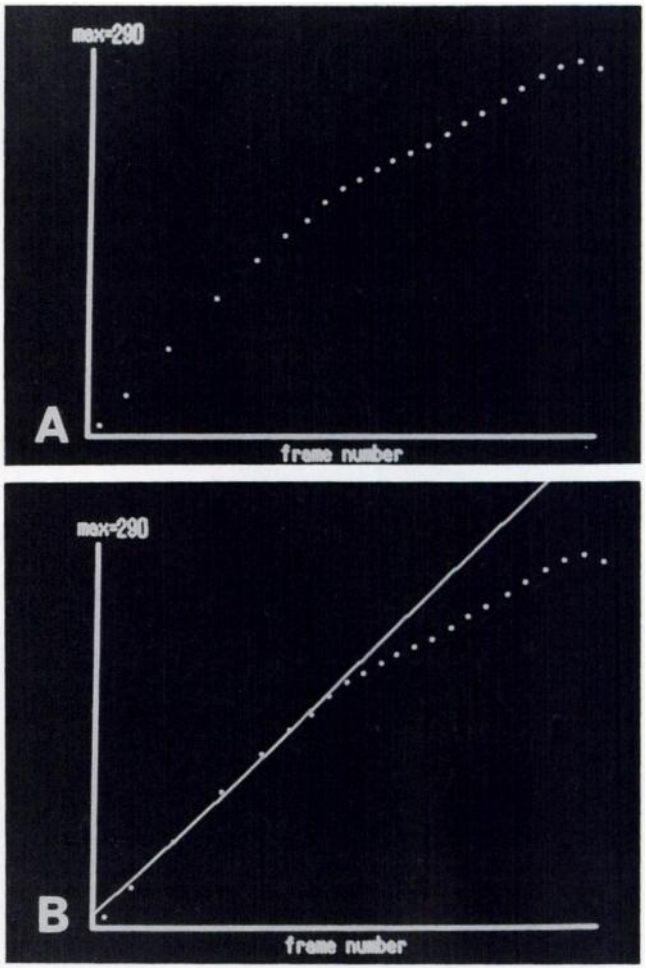

FIGURE 5. (A) A graph in which C(t)/E × B(t) is plotted on the y-axis against that on the x-axis, with relative values on both axes. The data were obtained after the second frame in the ROI placed over a cerebral hemisphere in the same subject as shown in Figures 1 and 4. (B) The straight line which reflects the linear relationship between both parameters.

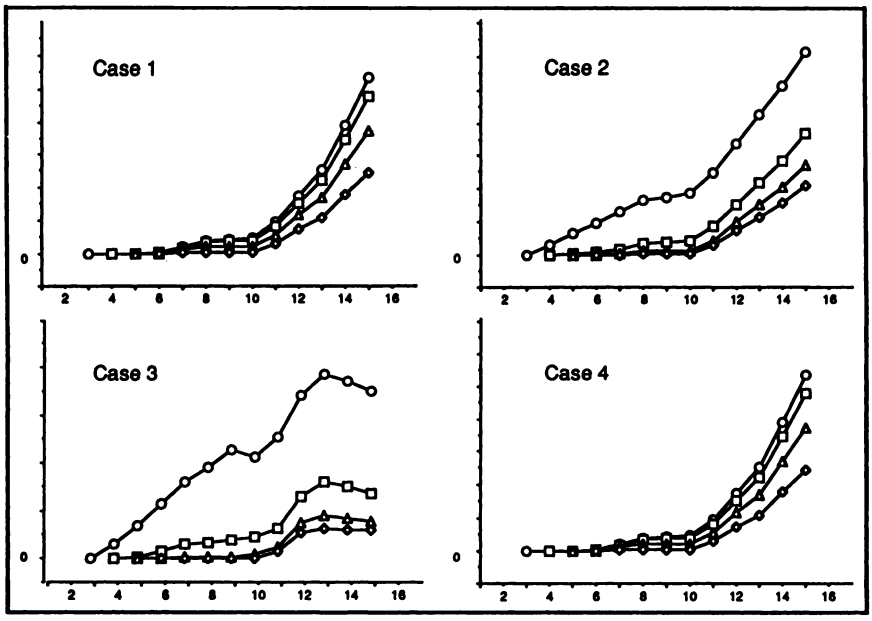

FIGURE 6. Changes of the least squares deviated values in linear fitting, starting from the second to fifth frames and ending at each frame up to the fifteenth in four healthy volunteers. The y-axis shows the relative values and the x-axis shows the frame where fitting ends for each graph (circles = fitting starts from the second frame; squares = starts from the third frame, triangles = starts from the fourth frame; and diamonds = starts from the fifth frame).

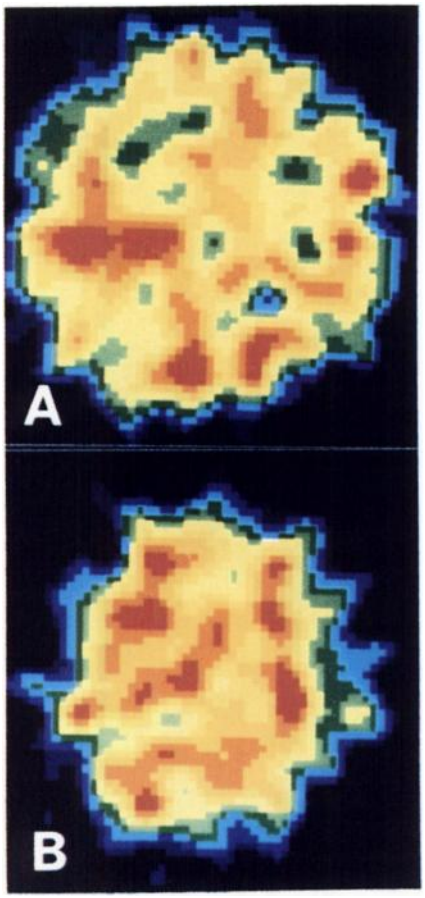

FIGURE 7. Functional maps of $rCBF_K$ obtained in a healthy volunteer for slices 55 mm (A) and 90 mm (B) above the OM line. The color scale indicates flow of 90 ml/100 g/min for red and 20 for blue.

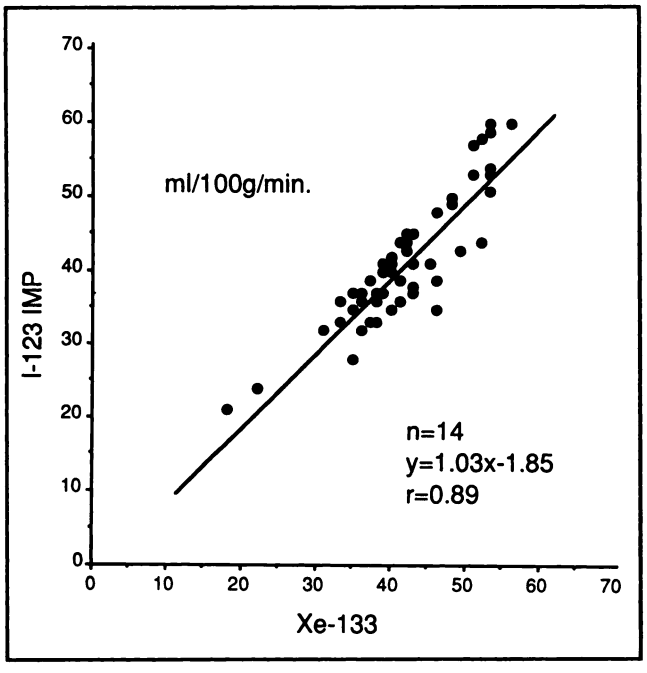

FIGURE 8. The relationship between $rCBF_K$ values and rCBF values obtained by ^{133}Xe inhalation SPECT studies for ROIs placed over the cerebral hemispheres in 14 patients.

As compared to the quantitative method using [^{123}I]IMP reported by Kuhl et al. (*9*) the one-point sampling of the arterial blood in our method is simpler and less invasive than the continuous withdrawal of blood through an arterial cannula. The postinjection image at 10 min or more is occasionally used for brain activity estimation in the method of Kuhl, when tomographic image obtained at 5 min does not provide adequate counts. In such cases, the washout of [^{123}I]IMP from the brain will result in underestimated rCBF values, as mentioned earlier.

REFERENCES

1. Winchell HS, Baldwin RM, Lin TH. Development of I-123-labelled amines for brain studies: localization of I-123 Iodophenylalkyl amines in rat brain. *J Nucl Med* 1980;21:940–946.
2. Winchell HS, Horst WD, Braun L, Oldendorf WH, Hattner R, Parker H. N-isopropyl-(I-123) p-iodoamphetamine: single-pass brain uptake and washout; binding to brain synaptosomes; and localization in dog and monkey brain. *J Nucl Med* 1980;21:947–952.
3. Rutland MD. A single injection technique for subtraction of blood background ^{131}I-hippuran renograms. *Br J Radiol* 1979;52:134–137.
4. Patlak CS, Blasberg RG, Fenstermacher JD. Graphical evaluation of blood-to-brain transfer constants from multiple-time uptake data. *J Cereb Blood Flow Metab* 1983;3:1–7.
5. Holman BL, Hill TC, Lee RGL, Zimmerman RE, Moore SC, Royal HD. Brain imaging with radiolabeled amines. In: Freeman LN, Weismann HS, eds. *Nuclear medicine annual.* New York: Raven Press; 1983:131–165.
6. Kanno I, Uemura K, Miura S, Miura S, Miura Y. HEADTOME: a hybrid emission tomograph for single photon and positron emission imaging of the brain. *J Comput Assist Tomogr* 1981;5:216–226.
7. Kanno I, Lassen NA. Two methods for calculating regional cerebral blood flow from emission computed tomography of inert gas concentrations. *J Comput Assist Tomogr* 1979;3:71–76.
8. Komatani A, Yamaguchi K, Sugai Y, et al. Assessment of demented patients by dynamic SPECT of inhaled Xe-133. *J Nucl Med* 1988;29:1621–1626.
9. Kuhl DE, Barrio JR, Huang S-C, et al. Quantifying local cerebral blood flow by N-isopropyl-(I-123) p-iodoamphetamine (IMP) tomography. *J Nucl Med* 1982;23:196–203.
10. Lassen NA, Henriksen L, Holm S. Cerebral blood-flow tomography: Xe-133 compared with isopropyl-amphetamine-iodine-123:concise communication. *J Nucl Med* 1983;24:17–21.
11. Hoffman EJ, Huang SC, Phelps ME. Quantitation in positron emission computed tomography: 1. effect of object size. *J Comput Assist Tomogr* 1979;3:299–308.
12. Yamamoto YL, Thompson CJ, Meyer E, Robertson JS, Feindel W. Dynamic positron emission tomography for study of cerebral hemodynamics in a cross section of the head using positron-emitting Ga-68-EDTA and Kr-77. *J Comput Assist Tomogr* 1977;1:43–56.
13. Frackowiak RSJ, Lenzi GL, Jones T, Heather JD. Quantitative measurement of regional cerebral blood flow and oxygen metabolism in man using O-15 and positron emission tomography: Theory, procedure, and normal values. *J Comput Assist Tomogr* 1980;4:727–760.
14. Baron JC, Bousser MG, Comar D, Sousaline F, Castaigne P. Noninvasive tomographic study of cerebral blood flow and oxygen metabolism in vivo. *Eur Neurol* 1981;20:273–284.
15. Huang SC, Carson RE, Hoffman EJ, et al. Quantitative measurement of local cerebral blood flow in humans by positron computed tomography and ^{15}O-water. *J Cereb Blood Flow Metabol* 1983;3:141–145.
16. Celesia GG, Polcyn RE, Holden JE, Nickles RJ, Koeppe RA, Gatley SJ: Determination of regional cerebral blood flow in patients with cerebral infarction. *Arch Neurol* 1984;41:262–267.
17. Olesen J, Paulson OB, Lassen NA: Regional cerebal blood flow in man determined by the initial slope of the clearance of intra-arterially injected Xe-133. *Stroke* 1971;2:519–540.
18. Orbist WD, Thompson HK, King CH, Wang HS. Determination of regional cerebral blood flow by inhalation of 133-Xe. *Circ Res* 1967;20:124–135.
19. Devous MD, Stokely EM, Chehabi HH, Bonte FJ. Normal distribution of

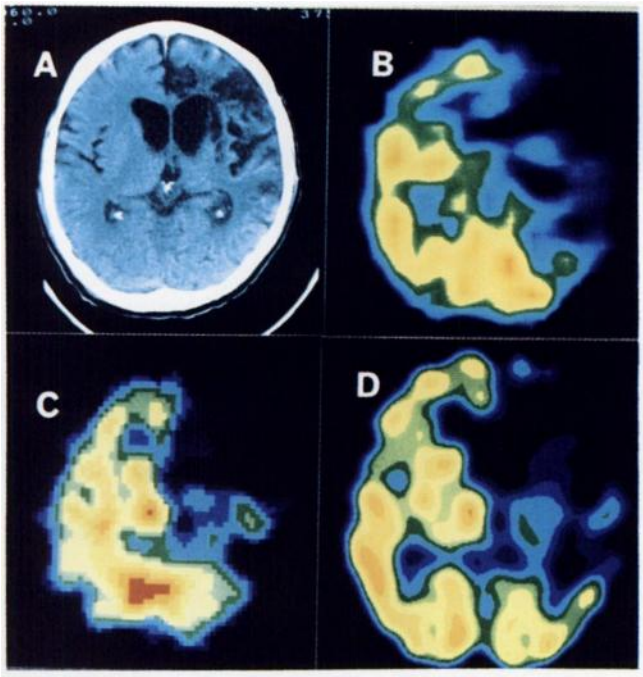

FIGURE 9. Three SPECT images obtained 55 mm above the OM line in a patient with right internal carotid artery occlusion and massive low density areas on brain CT (Subject 8). (A) Brain CT. (B) rCBF images obtained with ^{133}Xe. (C) The functional map obtained by our method. (D) The conventional [^{123}I]IMP image.

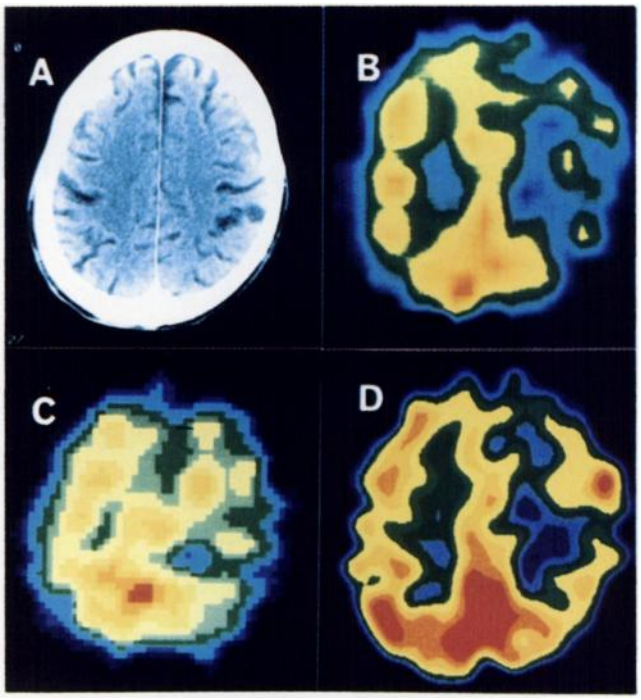

FIGURE 10. Three SPECT images obtained 90 mm above OM the line in a case of the right internal carotid artery occlusion without massive low density areas on brain CT (Patient 12). (A) Brain CT. (B) rCBF images obtained with ^{133}Xe. (C) The functional map obtained by our method. (D) The conventional [^{123}I]IMP image.

regional cerebral blood flow measured by dynamic single-photon emission tomography. *J Cereb Blood Flow Metab* 1986;6:95–104.

20. Lauritzen M, Henriksen L, Lassen NA. Regional cerebral blood flow during rest and skilled hand movements by xenon-133 inhalation and emission tomography. *J Cereb Blood Flow Metab* 1981;1:385–389.
21. Lenzi GL, Frackowiak RSJ, Lones T. Cerebral oxygen metabolism and blood flow in human cerebral ischemic infarction. *J Cereb Blood Flow Metab* 1982;2:321–335.
22. Lassen NA, Henriksen L, Paulson O: Regional cerebral blood flow in stroke by Xe-133 inhalation and emission tomography. *Stroke* 1981;12:284–288.
23. Takeshita G, Toyama H, Nakane K, et al. Minor changes in regional cerebral blood flow revealed by the early distribution of I-123 IMP in brain. *Radiation Med* 1991;9:196–201.